Priority Report

Cancer Research

Kras and *Tp53* Mutations Cause Cholangiocyte- and Hepatocyte-Derived Cholangiocarcinoma

Margaret A. Hill[1,2], William B. Alexander[1,2], Bing Guo[1,2], Yasutaka Kato[5,6], Krushna Patra[5,6], Michael R. O'Dell[2], Matthew N. McCall[1,3], Christa L. Whitney-Miller[4], Nabeel Bardeesy[5,6], and Aram F. Hezel[1,2]

Abstract

Intrahepatic cholangiocarcinoma (iCCA) is a primary liver cancer epidemiologically linked with liver injury, which has poorly understood incipient stages and lacks early diagnostics and effective therapies. While iCCA is conventionally thought to arise from the biliary tract, studies have suggested that both hepatocytes and biliary cells (cholangiocytes) may give rise to iCCA. Consistent with the plasticity of these cell lineages, primary liver carcinomas exhibit a phenotypic range from hepatocellular carcinoma (HCC) to iCCA, with intermediates along this spectrum. Here, we generated mouse models to examine the consequence of targeting mutant *Kras* and *Tp53*, common alterations in human iCCA, to different adult liver cell types. Selective induction of these mutations in the $SOX9^+$ population, predominantly consisting of mature cholangiocytes, resulted in iCCA emerging from premalignant biliary intraepithelial neoplasia (BilIN). In contrast, adult hepatocytes were relatively refractory to these mutations and formed rare HCC. In this context, injury accelerated hepatocyte-derived tumorigenesis and promoted a phenotypic switch to iCCA. BilIN precursor lesions were absent in the hepatocyte-derived iCCA models, pointing toward distinct and direct emergence of a malignant cholangiocytic phenotype from injured, oncogenically primed hepatocytes. *Tp53* loss enhanced the reprogramming of hepatocytes to cholangiocytes, which may represent a mechanism facilitating formation of hepatocyte-derived iCCA. Overall, our work shows iCCA driven by *Kras* and *Tp53* may originate from both mature cholangiocytes and hepatocytes, and factors such as chronic liver injury and underlying genetic mutations determine the path of progression and resulting cancer phenotype.

Significance: The histopathogenesis of biliary tract cancer, driven by *Tp53* and *Kras* mutations, can be differentially impacted by the cell of origin within the mature liver as well by major epidemiologic risk factors. *Cancer Res; 78(16); 4445–51.* ©*2018 AACR.*

Introduction

Intrahepatic cholangiocarcinoma (iCCA) is a lethal primary liver cancer that exhibits histologic features of the biliary tract and commonly harbors mutations in *IDH1/2*, *BAP1*, *KRAS*, *TP53*, *SMAD4*, and *ARID1A* (1, 2). Epidemiologic associations include conditions affecting the biliary compartment (e.g., primary sclerosing cholangitis and liver fluke infection) as well as the hepatocellular compartment (e.g., hepatitis B and C, and cirrhosis; ref. 3). In light of its histologic semblance, the mature cholangiocyte has traditionally been the assumed cell of origin in iCCA. However, the existence of mixed hepatocellular/cholangiocarcinoma (HCC-iCCA) tumors and the association of iCCA with chronic hepatocellular injury suggest the possibility of other cell types giving rise to iCCA including hepatocytes. Studies using transgenic mice have demonstrated that iCCA can develop from cholangiocytes; however, in the setting of severe carcinogenic injury or genetic activation of Notch signaling, a driver of biliary differentiation, iCCA can also arise from hepatocytes (4–7). This observation is consistent with models of acute liver injury in which hepatocytes can be reprogrammed to assume a biliary phenotype, a process that requires Notch activation (8, 9). The genetic and physiologic contexts in which this hepatocyte plasticity is relevant to iCCA remain to be fully understood.

In this study, we tested the oncogenic impact of targeting *Kras* and *Tp53* mutations to the adult liver compartment. In mature hepatocytes, these mutations only promoted iCCA in the context of liver injury. In contrast, the $SOX9^+$ compartment consisting predominantly of cholangiocytes was highly sensitive to iCCA development driven by these mutations. Moreover, only the latter model was associated with the multistage progression of premalignant biliary iCCA precursors, suggesting distinct premalignant lesions that are dictated by the cell of origin underlying iCCA pathogenesis. Finally, our results suggest that hepatocyte-

[1]Department of Biomedical Genetics, University of Rochester Medical Center, Rochester, New York. [2]Department of Medicine, Hematology/Oncology, Wilmot Cancer Institute, University of Rochester Medical Center, Rochester, New York. [3]Department of Biostatistics and Computational Biology, University of Rochester Medical Center, Rochester, New York. [4]Department of Pathology and Laboratory Medicine University of Rochester Medical Center, Rochester, New York. [5]Cancer Center, Massachusetts General Hospital, Boston, Massachusetts. [6]Department of Medicine, Harvard Medical School, Boston, Massachusetts.

Note: Supplementary data for this article are available at Cancer Research Online (http://cancerres.aacrjournals.org/).

M.A. Hill and W.B. Alexander contributed equally to this article.

Corresponding Author: Aram F. Hezel, Wilmot Cancer Institute, University of Rochester School of Medicine, 300 Elmwood Avenue, Rochester, NY 14642. Phone: 585-273-4150; Fax: 585-276-0337; E-mail: Aram_Hezel@URMC.Rochester.edu

doi: 10.1158/0008-5472.CAN-17-1123

to-cholangiocyte reprogramming serves as a barrier to *KRAS*-driven iCCA development and that *TP53* is a critical regulator of this process.

Materials and Methods

Mice

Mice were of mixed genetic background. All mouse strains (*Alb-Cre*, *Sox9-Cre^{ERT2}*, *Kras$^{LSL-G12D}$*, and *Tp53^{f}*) used have been studied previously. Mice were fed 0.1% DDC (3,5-diethoxycarbonyl-1,4-dihydrocollidine) diet for 2 weeks to 2 months, depending on the experiment (Custom Animal Diets, AD5001). In survival studies, mice were monitored for signs of illness including abdominal bloating, diminished activity, and/or poor grooming.

Tamoxifen and AAV8 injections

To generate hepatocyte-specific mutations for experiments relating to Fig. 1 and Supplementary Fig. S1, mice 10–25 weeks old were injected with 2.5×10^{11} viral AAV8-TBG-Cre particles via tail-vein injection or retro-orbital injection. To generate hepatocyte-specific mutations for experiments relating to Fig. 4, mice 8–12 weeks old were injected with 2.5×10^{11} viral AAV8-TBG-Cre particles via retro-orbital injection. To generate mutations in the SOX9^{+} compartment, *Sox9-Cre^{ERT2}* mice were injected intraperitoneally with 100 mg/kg tamoxifen dissolved in corn oil every other day for 6 days.

Histology

Tissue was fixed in 10% formalin, paraffin embedded, cut into 4-μm sections, and put on slides. Deparaffinized sections underwent antigen retrieval in citrate buffer (Dako) for 30 minutes, blocked for 4 minutes in Background Sniper (Biocare Medical). Sections were incubated with primary antibodies overnight at 4°C and secondary antibodies for 2 hours at room temperature, then incubated with ABC complex (Vectastain) and VECTOR Red (Vector Laboratories) or HSS-HRP and DAB (Vector Laboratories), then stained with hematoxylin. Immunofluorescence sections were incubated with Hoechst for 45 minutes at room temperature. Antibodies: anti-PanCK (Dako #Z0622), anti-hepatocyte (Biocare Medical #166), anti-JAG1 (Santa Cruz Biotechnology #8303), anti-KRT19 (DSHB), anti-WNT7B (Novus

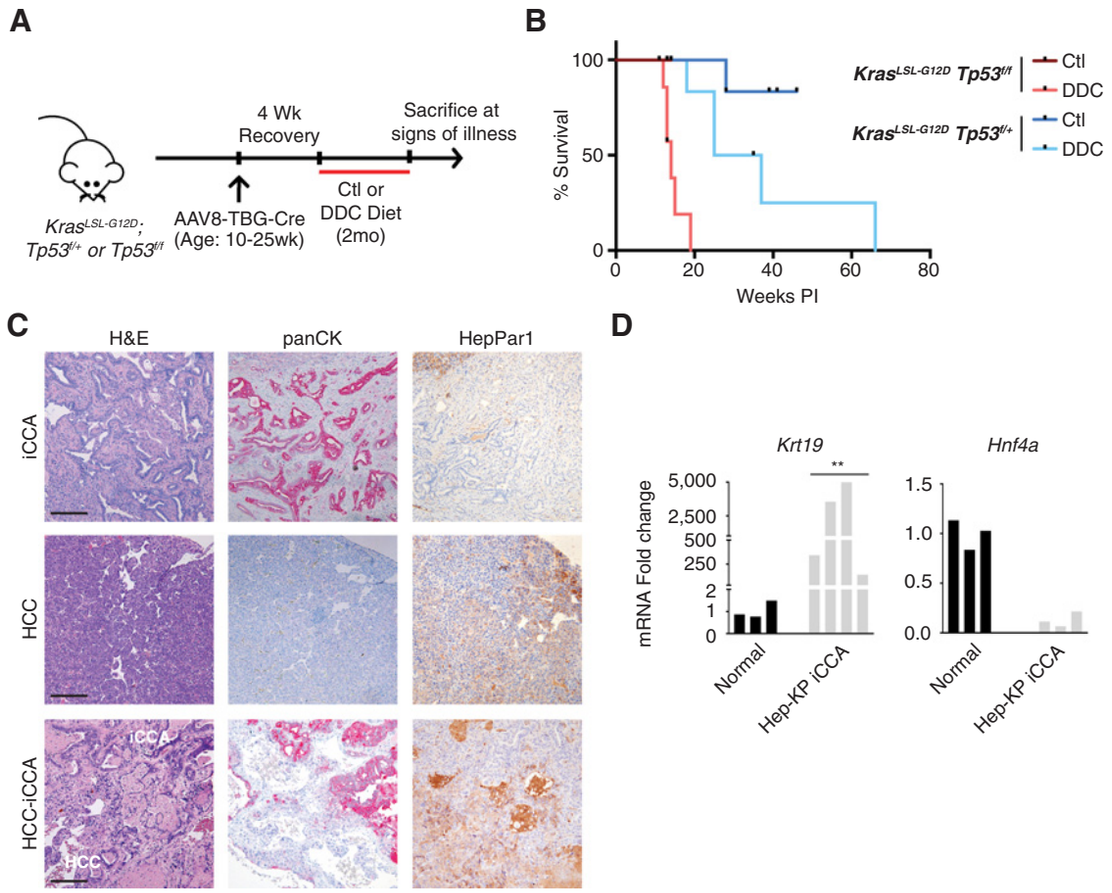

Figure 1.

Targeting *Kras* and *Tp53* mutations to the hepatocyte compartment promotes iCCA in the setting of injury. **A,** Hepatocyte-specific Cre-mediated recombination was induced in *Kras$^{LSL-G12D}$;Tp53$^{f/f}$* and *Kras$^{LSL-G12D}$;Tp53$^{f/+}$* mice ages 10–25 weeks by injection with AAV8-TBG-Cre. Mice were provided control (Ctl) or DDC diet for 2 months and followed until signs of illness. **B,** Liver tumor–specific survival of Hep-KP mice. **C,** Representative images of hematoxylin and eosin (H&E) staining and IHC for panCK and HepPar1 on liver tumors from DDC-treated Hep-KP mice. Scale bars, 200 μm. **D,** qPCR analyses for biliary marker *Krt19* and hepatocyte marker *Hnf4a* in normal liver and Hep-KP–derived iCCA. **, $P < 0.01$.

Biologicals #NBP1–59564), anti-GFP (Cell Signaling Technology #2956), biotinylated anti-rabbit (Vector BA-1000), Alexa Fluor 488 α-rabbit (Thermo Scientific A-11008), and Alexa Fluor 555α-rat (Thermo Scientific A-21434).

qPCR

RNA was extracted from frozen liver tissue using the RNeasy Mini Kit (Qiagen). cDNA was created using a high-capacity cDNA Reverse Transcriptase Kit (Applied Biosystems). All qPCR reactions were performed in triplicate, using SYBR Green Master Mix (Bio-Rad). Expression level was normalized to RhoA. The following primer sets were used. *Axin2*: 5′-GCCAATGGCCAAGTGTCTCT-3′ and 5′-GCGTCATCTCCTTGGGCA-3′; *Dll1*: 5′-GATGGATCTCTGCGGCTCTTC-3′ and 5′-GCACCGGCACAGGTAAGAGT-3′; *Hes1*: 5′-AAAGCCTATCATGGAGAAGAGGCG-3′ and 5′-GGAATGCCGGGAGCTATCTTTCTT-3′; *Hey1*: 5′-ACACTGCAGGAGGGAAAGGTT-3′ and 5′-CAAACTCCGATAGTCCATAGCCA-3′; *Hnf4a*: 5′-GGTAGGGGAGAATGCGACTC-3′ and 5′-AAACTCCAGGGTGGTGTAGG-3′; *Jag1*: 5′-CCCACGTGTTCCACAAACATC-3′ and 5′-CCATGGGAACAGTTATTTGGAGA-3′; *Krt19*: 5′-TGCTGGATGAGCTGACTCTG-3′ and 5′-AATCCACCTCCACACTGACC-3′; *Lef1*: 5′-CCCACACGGACAGTGACCTA-3′ and 5′-TGGGCTCCTGCTCCTTTCT-3′; *Wnt10a*: 5′-TGGAGACTCGGAACAAAGTC-3′ and 5′-AGCTTCCGACGGAAAGCTTC-3′; and *Wnt7b*: 5′-GGTGTGGCAGTGTACCTGCAA-3′ and 5′-GTGAAGACCTCGGTGCGCT-3′.

Statistical analysis

Statistics for qPCR were calculated on the raw, log-scale data using a Welch *t* test. For visualization, data were represented as fold change and normalized to control liver samples. Statistics for Kaplan–Meier analysis were calculated according to the log-rank (Mantel–Cox) test. To analyze Fig. 4, 15 random portal fields per mouse were independently quantified by three blinded observers for the proportion of $KRT19^+$ cells that were YFP^+; the average of these three values was used for statistical analysis.

Study approval

All animal studies were conducted in accordance with the Association for Assessment and Accreditation of Laboratory Animal Care–accredited University Committee on Animal Resources.

Results and Discussion

We previously established that targeting *Kras* and *Tp53* mutations to the mouse liver using the *Alb-Cre* transgene (*Alb-Cre*; $Kras^{LSL\text{-}G12D}$;$Tp53^{f/f}$or $Tp53^{f/+}$; AKP model) results in development of tumors with a histologic spectrum ranging from exclusively iCCA to exclusively hepatocellular carcinoma (HCC; ref. 10). The *Alb-Cre* allele recombines floxed alleles in both hepatocytes and cholangiocytes, beginning in late embryogenesis (11). To evaluate the response of mature hepatocytes to these genetic alterations, we employed intravenous injection of an adeno-associated virus with hepatocyte-specific tropism to deliver Cre recombinase expressed under the hepatocyte-specific thyroid-binding globulin promoter (AAV8-TBG-Cre; refs. 8, 9). Lineage tracing using a $Rosa^{LSL\text{-}YFP}$ reporter allele revealed efficient recombination in hepatocytes, and the absence of YFP^+/$KRT19^+$ cells confirmed that this strategy does not target cholangiocytes (Supplementary Fig. S1). Adult $Kras^{LSL\text{-}G12D}$;$Tp53^{f/f}$ ($n = 4$) or $Kras^{LSL\text{-}G12D}$;$Tp53^{f/+}$ ($n = 6$) mice were injected with virus and monitored until signs of illness (Hep-KP mice; Fig. 1A and B). While each animal had visible tumors at necropsy, all were extrahepatic (lung and soft tissue). Moreover, histologic analysis revealed only a single microscopic focus of early HCC among the first 10 mice surveyed (Supplementary Table S1). Thus, mature hepatocytes are relatively refractory to *Kras–Tp53* mutations as compared with other tissues where AAV8-TBG-Cre exhibits ectopic activity.

Liver injury is an important risk factor for both iCCA and HCC and can precipitate hepatic cellular plasticity (3, 8, 12). Furthermore, the signaling pathways required to facilitate such transdifferentiation events are implicated in iCCA pathogenesis (5, 8, 13, 14). On the basis of these considerations, we evaluated the impact of liver injury on mature *Kras–Tp53* mutant hepatocytes using the AAV8-TBG-Cre model. The DDC diet is a noncarcinogenic liver injury model that causes ductular reaction, fibrosis, and inflammation (4, 15). Following administration of AAV8-TBG-Cre and a recovery period, adult $Kras^{LSL\text{-}G12D}$;$Tp53^{f/f}$ ($n = 7$) or $Kras^{LSL\text{-}G12D}$; $Tp53^{f/+}$ ($n = 6$) mice were placed on DDC diet for 2 months and then monitored until signs of illness (Fig. 1A). In this cohort, 12 of 13 mice were sacrificed due to significant liver tumor burden (range, 12–66 weeks postinjection), with several mice exhibiting multiple discrete liver tumors (Fig. 1B). Histologic examination of the 18 liver tumors revealed iCCA ($n = 7$), HCC ($n = 7$), and mixed iCCA–HCC with discernible zones of histologic transition ($n = 4$; Fig. 1C; Supplementary Table S1). We verified that iCCA and HCC had the expected IHC staining profiles for panCK and HepPar1 (Fig. 1C). Moreover, qRT-PCR confirmed expression of the ductal marker *Krt19* and loss of the hepatocyte marker *Hnf4a* in Hep-KP–derived iCCAs (Fig. 1D). Similar results were observed in the AKP model, where the DDC diet markedly accelerated tumor development (median survival, 54 vs. 34 weeks) and shifted the tumor spectrum from one of equal proportions of HCC, iCCA, and mixed HCC-iCCA to one with all tumors consisting of iCCA or mixed HCC-iCCA phenotypes (Supplementary Fig. S2A–S2D). Thus, DDC treatment both sensitizes *Kras–Tp53*–mutant hepatocytes to malignant transformation and confers a phenotypic switch specifically favoring an iCCA pathology.

Next, we assessed the sensitivity of the mature ductal compartment to *Kras–Tp53* mutations by generating a cohort of $Sox9\text{-}Cre^{ERT2}$; $Kras^{LSL\text{-}G12D}$;$Tp53^{f/f}$ mice (SOX9-KP model; ref. 16). The $Sox9\text{-}Cre^{ERT2}$ transgene enables recombination of floxed alleles in the liver bile ducts, while largely sparing the hepatocytes (Supplementary Fig. S3A and S3B), as well as several extrahepatic cell types. All SOX9-KP mice developed liver masses following tamoxifen injection (average latency, 30 weeks; Fig. 2A and B). Histologic analyses revealed that 7 of 9 mice had iCCA with characteristic ductal and glandular features and positive panCK staining, whereas a single animal developed HCC (Fig. 2C; Supplementary Table S2). Notably, adjacent liver to iCCA exhibited extensive ductular reactions and stromal proliferation, as well as dysplastic, panCK-positive biliary lesions resembling biliary intraepithelial neoplasia (BilIN), an established precursor of human iCCA (Fig. 2C). Thus, the biliary compartment is readily transformed by *Kras* and *Tp53* mutations, which generate a phenotype consisting of staged ductal precursor lesions and iCCA development.

This expansion of premalignant biliary precursors was specific to the SOX9-KP model. Despite the prominent formation

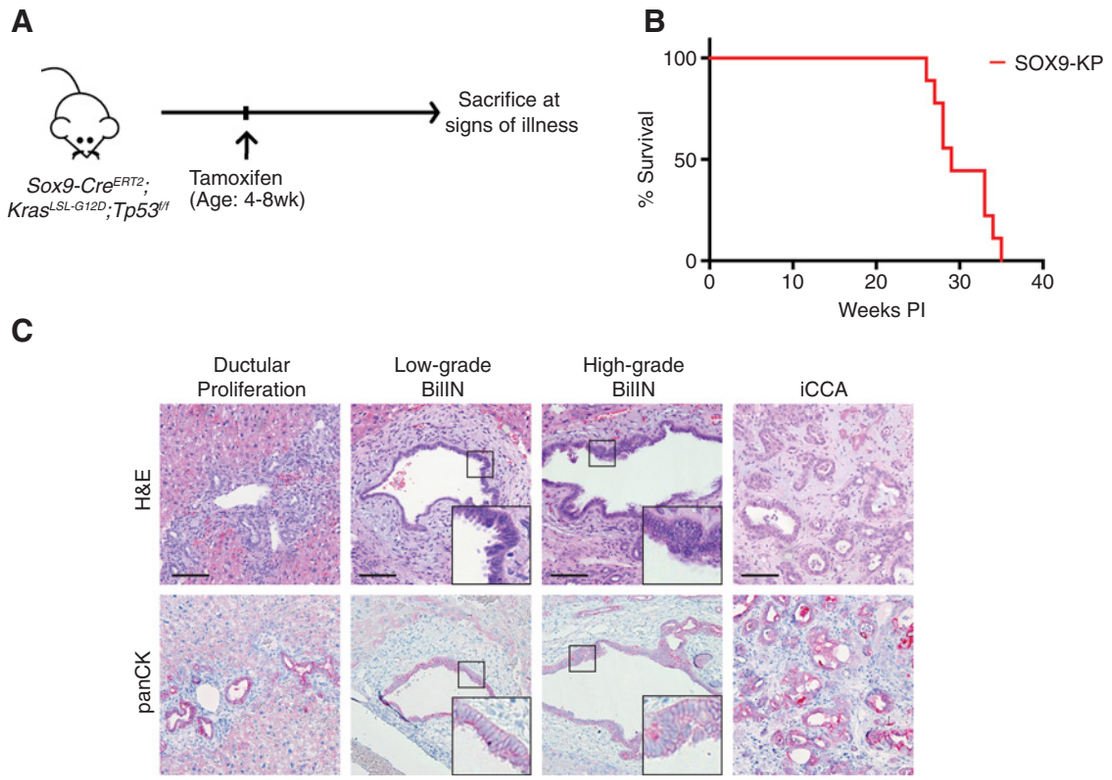

Figure 2.

Targeting *Kras* and *Tp53* mutations to the SOX9$^+$ compartment promotes BilIN and iCCA. **A,** Cre-mediated recombination was induced in *Sox9-Cre*^{ERT2};*Kras*$^{LSL-G12D}$;*Tp53*$^{f/f}$ mice via tamoxifen injections between ages 4 and 8 weeks, and mice were followed for signs of illness ($n = 9$ mice). **B,** Kaplan–Meier analysis displaying time until illness of SOX9-KP mice. **C,** Hematoxylin and eosin (H&E) and panCK IHC staining of liver sections revealing progressive spectrum of biliary lesions in the SOX9-KP model. Scale bars, 100 μm. Insets show ×3 magnification view.

of iCCA in the Hep-KP and AKP-DDC models, there was a virtual absence of associated BilIN lesions. Serial analysis of DDC-treated AKP-mice prior to signs of illness further corroborated these findings. In particular, among the cohort analyzed (4 mice), there was only a single case where an isolated focus of iCCA was found in zone three of the liver, distant from the bile ducts without evidence of any ductal metaplasia (Supplementary Fig. S2D). Thus, evident biliary precursor lesions do not precede development of iCCA from hepatocytes in this model, suggesting that the observed phenotypic shift may represent the direct transformation and transdifferentiation of hepatocytes. Overall, these data reveal that the tumor-suppressive barriers and steps of histopathologic progression are distinct in iCCA arising from either liver cell lineage.

To understand the signaling events contributing to hepatocyte (Hep-KP) and biliary (SOX9-KP)–derived iCCA, we examined the Notch and Wnt pathways, which are implicated in liver cell fate decisions and in the sustained growth of iCCA (8, 17–20). Hep-KP–derived iCCAs show high expression of the Notch ligand *Jag1* ($P = 0.005$) and target genes *Hey1* ($P = 0.009$), and *Hes1* ($P = 0.026$) compared with nonmalignant liver (Fig. 3A). Furthermore, in contrast to hepatocytes in a DDC injured liver, which show minimal JAG1 staining compared with adjacent biliary cells, and mirroring the SOX9-KP iCCA model, Hep-KP iCCA shows costaining of JAG1 with the biliary marker KRT19 in the malignant epithelium, indicating expression of JAG1 is acquired during hepatocyte-to-iCCA transformation (Fig. 3B). Among most of the HCC–iCCA transitional zones, JAG1 staining correlates with KRT19 staining, suggesting Notch signaling may drive differentiation towards a biliary-like fate (Supplementary Fig. S4A). Evaluation of the Wnt pathway revealed Wnt ligands *Wnt7b* ($P = 0.001$) and *Wnt10a* ($P = 0.001$), and the target gene *Lef1* ($P = 0.096$) is also expressed at high levels in Hep-KP–derived iCCAs, reflecting observations in biliary-derived iCCA (Supplementary Fig. S4B). Furthermore, immunofluorescence reveals strong WNT7B staining in the KRT19 compartment, as well as in occasional stromal cells, consistent with previous observations (Supplementary Fig. S4C; ref. 19). Together, these data indicate that Notch signaling is activated during hepatocyte-to-iCCA transformation, which may promote the biliary differentiation characteristic of iCCA. Furthermore, Hep-KP and SOX9-KP–derived iCCAs exhibit activity in Notch and Wnt signaling, suggesting they may share similar biologic programming regarding these important targetable pathways.

Having established that hepatocyte-derived cancer can acquire biliary identity in the setting of *Kras* and *Tp53* mutations, we sought to determine whether the capacity to transdifferentiate is determined by the underlying mutational context. It was previously demonstrated that deletion of *Tp53* in the liver promotes undifferentiated tumors that express the stem cell marker *Nestin* (21). Furthermore, *Kras* mutations in the

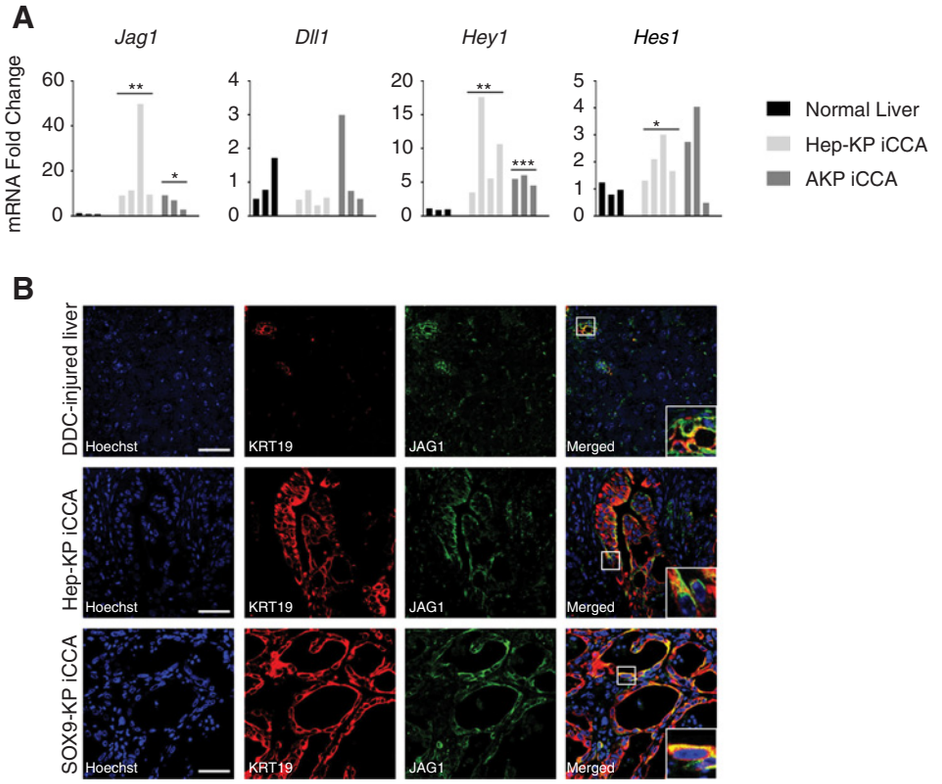

Figure 3.

Hep-KP–derived iCCA exhibits activity in Notch signaling. **A,** qPCR analyses for Notch ligands *Jag1* and *Dll1*, and Notch target genes *Hes1* and *Hey1*. **B,** Immunofluorescence for the Notch ligand JAG1 and the biliary marker KRT19 in DDC-injured liver demonstrating expression in the KRT19$^+$ biliary compartment and in iCCA in both SOX9 and Hep-KP models. Scale bars, 50 μm. Insets show ×3 magnification view. *, $P < 0.05$; **, $P < 0.01$; ***, $P < 0.001$.

absence of *Tp53* mutations can drive HCC (7, 10, 22). Taken together, these observations suggest that inactivation of *Tp53* in hepatocytes may be critical in enabling biliary differentiation associated with iCCA; therefore, we sought to specifically evaluate the role of *Tp53* in the process of hepatocyte-to-cholangiocyte reprogramming in states of injury when a small proportion of resulting KRT19$^+$ biliary-like cells may be derived from hepatocytes (8). We hypothesized that the deletion of *Tp53* in hepatocytes could lead to increased transdifferentiation events, and therefore, more hepatocyte-derived KRT19$^+$ cells. To test this, mice ($n = 4$/cohort) carrying *Tp53*$^{f/f}$ or *Tp53*$^{+/+}$ and the *Rosa26*$^{LSL\text{-}YFP}$ reporter were injected with AAV8-TBG-Cre to generate hepatocyte-specific mutations and lineage trace this compartment. Following 2 weeks of recovery, mice were provided a 2-week DDC diet to induce injury and provoke transdifferentiation (Fig. 4A). Quantifications of randomly imaged portal fields for the percentage of hepatocyte-derived cholangiocytes (YFP$^+$/KRT19$^+$) relative to the total number of cholangiocytes (KRT19$^+$) revealed over a 5-fold increase, from 0.6% in *Tp53*$^{+/+}$ to 3.4% in the *Tp53*$^{f/f}$ cohort ($P = 0.05$, Welch *t* test; Fig. 4B). This substantial increase in hepatocyte-derived cholangiocytes is most likely due to an increased rate of transdifferentiation rather than preferential expansion of *Tp53*-null cholangiocytes, because targeting deletion of *Tp53* to cholangiocytes as well as hepatocytes via *Alb-Cre* did not increase cholangiocyte expansion following DDC injury (Supplementary Fig. S5A and S5B). Furthermore, we observe only a relatively small increase in Ki67 labeling in *Tp53*$^{f/f}$ versus *Tp53*$^{+/+}$ AAV8-TBG-Cre–targeted hepatocytes post-DDC injury (Supplementary Fig. S6A and S6B), suggesting the 5-fold change we observe in costaining cells is unlikely to be caused by this modest proliferative advantage. Thus, we find that *Tp53* restricts hepatocyte-to-cholangiocyte reprogramming and offers a potential mechanism by which *Tp53* mutation enables hepatocyte-derived iCCA.

In summary, we show that mature cholangiocytes and hepatocytes can both give rise to iCCA in the setting of *Kras* and *Tp53* mutations, and liver injury plays a key role in both priming hepatocytes for malignant transformation and facilitating iCCA development. Importantly, we show that the cell of origin may dictate the histopathologic route to iCCA, with cholangiocyte-derived iCCA uniquely being associated with BilIN precursor lesions. Finally, our data indicate that hepatocyte-to-cholangiocyte reprogramming is an important barrier to tumorigenesis and is restricted by *Tp53* function.

The appreciation of cellular plasticity in liver regeneration has led to reconsideration of cellular origins of HCC and iCCA (5, 8). Here, we demonstrate how the interplay between the cellular compartment, oncogenic mutations, and presence or absence of tissue injury determines the histopathologic paths to cancer and the resulting tumor phenotype (4, 10, 22). In the case of *Kras* and *Tp53* mutations, coexisting mutations in human tumors, there are distinct barriers and premalignant precursor lesions depending on whether the cholangiocytes or hepatocytes are targeted. In ductal cells, such mutations drive multistage progression of ductal lesions to iCCA. *Kras–Tp53*–mutant hepatocytes, however, can be pushed toward this same malignant fate in the setting of injury but without evidence of ductal precursor lesions. *Tp53* may play a key role in enabling hepatocyte-derived iCCA in this context. *TP53* has been shown to control plasticity in a number of different cellular contexts and is known to control stemness qualities among primary liver

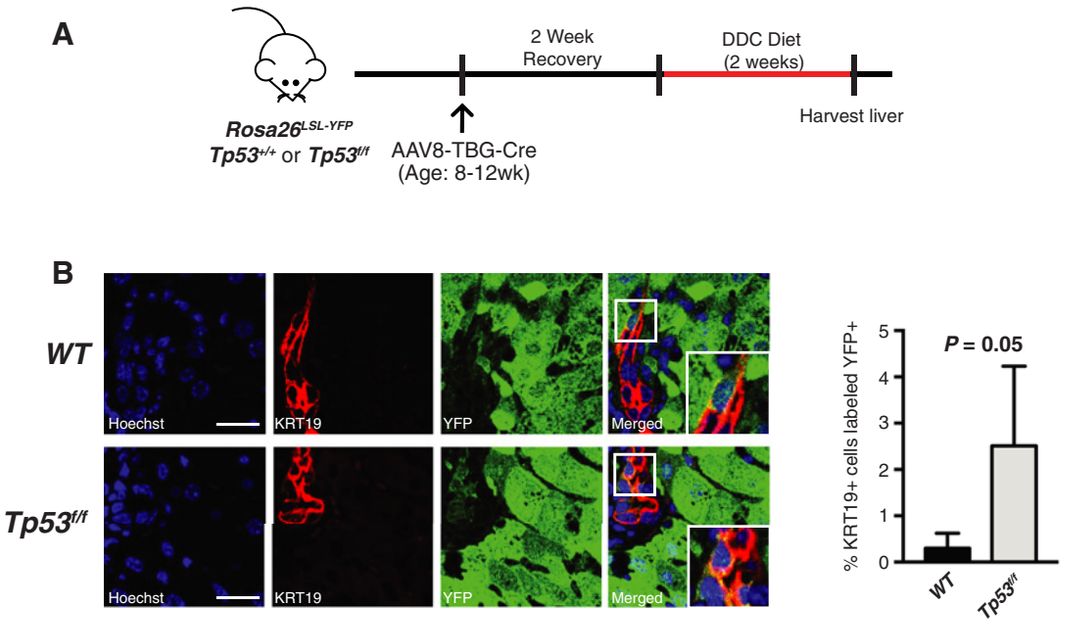

Figure 4.

Tp53 restricts hepatocyte-to-cholangiocyte reprogramming. **A,** $Tp53^{f/f}$ or $Tp53^{+/+}$ mice with the $Rosa26^{LSL\text{-}YFP}$ reporter were injected with AAV8-TBG-Cre to induce hepatocyte-specific Cre-mediated recombination. After recovery, mice were put on a 2-week DDC diet to induce hepatocyte-to-cholangiocyte reprogramming. **B,** Quantification of $YFP^+/KRT19^+$ cells. Representative images are shown of $YFP^+/KRT19^+$ cells and adjacent $YFP^-/KRT19^+$ cells ($n = 4$ mice/cohort, 15 portal fields/mouse; $P = 0.05$ by Welch t test). Scale bars, 25 μm. Insets show ×3 magnification view.

cancers via regulation of Nestin (21, 23). We now identify a *Tp53*-dependent inhibition of hepatocyte-to-cholangiocyte reprogramming as an important mechanism suppressing the development of hepatocyte-derived iCCA.

Overall, iCCAs deriving from distinct cells of origin may have differences in prognosis and therapeutic susceptibility, warranting investigation into associated biomarkers. Our models point to the potential impact of differing cells-of-origin on disease biology; in particular, the prevalence of precursor lesions in each model could be relevant for screening and prevention strategies. Furthermore, although each has a unique route of histologic progression to iCCA, cholangiocyte-derived and hepatocyte-derived iCCA both exhibit activity in Notch and Wnt signaling, suggesting similar biologic programming in these targetable pathways, regardless of the cell of origin.

Disclosure of Potential Conflicts of Interest

No potential conflicts of interest were disclosed.

Authors' Contributions

Conception and design: M.A. Hill, W.B. Alexander, N. Bardeesy, A.F. Hezel
Development of methodology: M.A. Hill, W.B. Alexander, A.F. Hezel
Acquisition of data (provided animals, acquired and managed patients, provided facilities, etc.): M.A. Hill, W.B. Alexander, B. Guo, Y. Kato, K. Patra, M.R. O'Dell, A.F. Hezel
Analysis and interpretation of data (e.g., statistical analysis, biostatistics, computational analysis): M.A. Hill, W.B. Alexander, B. Guo, K. Patra, M.R. O'Dell, M.N. McCall, C.L. Whitney-Miller, N. Bardeesy, A.F. Hezel
Writing, review, and/or revision of the manuscript: M.A. Hill, W.B. Alexander, C.L. Whitney-Miller, N. Bardeesy, A.F. Hezel
Administrative, technical, or material support (i.e., reporting or organizing data, constructing databases): M.A. Hill, W.B. Alexander, M.R. O'Dell, A.F. Hezel
Study supervision: N. Bardeesy, A.F. Hezel

Acknowledgments

A.F. Hezel is supported by the NCI (1R01CA172302) and For Pete's Sake Golf Tournament in memory of Pete Osterling and N. Bardeesy by the NIH (P01 CA117969-07, R01 CA133557-05, and P50CA1270003), Gallagher Endowed Chair in Gastrointestinal Cancer Research, and TargetCancer Foundation.

The costs of publication of this article were defrayed in part by the payment of page charges. This article must therefore be hereby marked *advertisement* in accordance with 18 U.S.C. Section 1734 solely to indicate this fact.

Received April 20, 2017; revised April 18, 2018; accepted May 30, 2018; published first June 5, 2018.

References

1. Nakamura H, Arai Y, Totoki Y, Shirota T, Elzawahry A, Kato M, et al. Genomic spectra of biliary tract cancer. Nat Genet 2015;47:1003–10.
2. Jusakul A, Cutcutache I, Yong CH, Lim JQ, Huang MN, Padmanabhan N, et al. Whole-genome and epigenomic landscapes of etiologically distinct subtypes of cholangiocarcinoma. Cancer Discov 2017;7:1116–35.
3. Banales JM, Cardinale V, Carpino G, Marzioni M, Andersen JB, Invernizzi P, et al. Expert consensus document: Cholangiocarcinoma: current knowledge and future perspectives consensus statement from the European Network for the Study of Cholangiocarcinoma (ENS-CCA). Nat Rev Gastroenterol Hepatol 2016;13:261–80.

4. Guest RV, Boulter L, Kendall TJ, Minnis-Lyons SE, Walker R, Wigmore SJ, et al. Cell lineage tracing reveals a biliary origin of intrahepatic cholangiocarcinoma. Cancer Res 2014;74:1005–10.
5. Fan B, Malato Y, Calvisi DF, Naqvi S, Razumilava N, Ribback S, et al. Cholangiocarcinomas can originate from hepatocytes in mice. J Clin Invest 2012;122:2911–5.
6. Sekiya S, Suzuki A. Intrahepatic cholangiocarcinoma can arise from Notch-mediated conversion of hepatocytes. J Clin Invest 2012;122:3914–8.
7. Ikenoue T, Terakado Y, Nakagawa H, Hikiba Y, Fujii T, Matsubara D, et al. A novel mouse model of intrahepatic cholangiocarcinoma induced by liver-specific Kras activation and Pten deletion. Sci Rep 2016;6:23899.
8. Yanger K, Zong Y, Maggs LR, Shapira SN, Maddipati R, Aiello NM, et al. Robust cellular reprogramming occurs spontaneously during liver regeneration. Genes Dev 2013;27:719–24.
9. Font-Burgada J, Shalapour S, Ramaswamy S, Hsueh B, Rossell D, Umemura A, et al. Hybrid periportal hepatocytes regenerate the injured liver without giving rise to cancer. Cell 2015;162:766–79.
10. O'Dell MR, Huang JL, Whitney-Miller CL, Deshpande V, Rothberg P, Grose V, et al. Kras(G12D) and p53 mutation cause primary intrahepatic cholangiocarcinoma. Cancer Res 2012;72:1557–67.
11. Xu X, Kobayashi S, Qiao W, Li C, Xiao C, Radaeva S, et al. Induction of intrahepatic cholangiocellular carcinoma by liver-specific disruption of Smad4 and Pten in mice. J Clin Invest 2006;116:1843–52.
12. Llovet JM, Zucman-Rossi J, Pikarsky E, Sangro B, Schwartz M, Sherman M, et al. Hepatocellular carcinoma. Nat Rev Dis Primers 2016;2:16018.
13. Kim W, Khan SK, Gvozdenovic-Jeremic J, Kim Y, Dahlman J, Kim H, et al. Hippo signaling interactions with Wnt/beta-catenin and Notch signaling repress liver tumorigenesis. J Clin Invest 2017;127:137–52.
14. Yimlamai D, Christodoulou C, Galli GG, Yanger K, Pepe-Mooney B, Gurung B, et al. Hippo pathway activity influences liver cell fate. Cell 2014;157:1324–38.
15. Fickert P, Stoger U, Fuchsbichler A, Moustafa T, Marschall HU, Weiglein AH, et al. A new xenobiotic-induced mouse model of sclerosing cholangitis and biliary fibrosis. Am J Pathol 2007;171:525–36.
16. Kopp JL, Dubois CL, Schaffer AE, Hao E, Shih HP, Seymour PA, et al. Sox9+ ductal cells are multipotent progenitors throughout development but do not produce new endocrine cells in the normal or injured adult pancreas. Development 2011;138:653–65.
17. Zong Y, Panikkar A, Xu J, Antoniou A, Raynaud P, Lemaigre F, et al. Notch signaling controls liver development by regulating biliary differentiation. Development 2009;136:1727–39.
18. Boulter L, Govaere O, Bird TG, Radulescu S, Ramachandran P, Pellicoro A, et al. Macrophage-derived Wnt opposes Notch signaling to specify hepatic progenitor cell fate in chronic liver disease. Nat Med 2012;18:572–9.
19. Boulter L, Guest RV, Kendall TJ, Wilson DH, Wojtacha D, Robson AJ, et al. WNT signaling drives cholangiocarcinoma growth and can be pharmacologically inhibited. J Clin Invest 2015;125:1269–85.
20. Guest RV, Boulter L, Dwyer BJ, Kendall TJ, Man T-Y, Minnis-Lyons SE, et al. Notch3 drives development and progression of cholangiocarcinoma. Pro Natl Acad Sci U S A 2016;113:12250–5.
21. Tschaharganeh DF, Xue W, Calvisi DF, Evert M, Michurina TV, Dow LE, et al. p53-dependent nestin regulation links tumor suppression to cellular plasticity in liver cancer. Cell 2014;158:579–92.
22. Saha SK, Parachoniak CA, Ghanta KS, Fitamant J, Ross KN, Najem MS, et al. Mutant IDH inhibits HNF-4a to block hepatocyte differentiation and promote biliary cancer. Nature 2014:513:110–14.
23. Jiang H, Xu Z, Zhong P, Ren Y, Liang G, Schilling HA, et al. Cell cycle and p53 gate the direct conversion of human fibroblasts to dopaminergic neurons. Nat Commun 2015;6:10100.